Some considerations on exponential flights

A. Zoia,[1, *] E. Dumonteil,[1] and A. Mazzolo[1]

[1] *CEA/Saclay, DEN/DM2S/SERMA/LTSD, Bât. 470, 91191 Gif-sur-Yvette Cedex, France*

In this paper we elucidate the relation between the Boltzmann equation, which governs the evolution of many random transport phenomena in Physics (such as the propagation of neutrons, or the migration of chemical and biological species), and the underlying stochastic process, the so-called *exponential flights*. After introducing a general framework for *d*-dimensional setups, we analyze in detail the case $d = 1, 2, 3$, and 4. In particular, we derive a number of exact or asymptotic results, providing a link between the space and time evolution of the transported particles, and the statistics of collisions each particle undergoes in a given bounded or unbounded, as well as scattering or absorbing domain. Monte Carlo simulations are performed so as to support our findings.

I. INTRODUCTION

Random walks are widely used in Physics so as to model the features of transport processes where the migrating (possibly massless) particle undergoes a series of random displacements as the effect of repeated collisions with the surrounding environment [1–4]. While much attention has been given to random walks on regular Euclidean lattices, and to the corresponding scaling limits, less has been comparatively devoted to the case where the direction of propagation can change continuously at each collision: for a review, see, e.g., [5]. Such processes, which have been named *random flights*, play nonetheless a prominent role in the description of, among others, neutron or photon propagation through matter [6–8], and chemical and biological species migration [9].

Within the simplest formulation of this model, which was originally proposed by Pearson (1905) and later extended by Kluyver (1906) and Rayleigh (1919) [5], it is assumed that particles perform random displacements ('flights') along straight lines, and that at the end of each flight (a 'collision' with the surrounding medium) the direction of propagation changes at random.

When the number of transported particles is much smaller than the number of the particles of the interacting medium, so that inter-particles collisions can be safely neglected, it is reasonable to assume that the probability of interacting with the medium is Poissonian. For the case of neutrons in a nuclear reactor, e.g., the ratio between the number of transported particles and the number of interacting nuclei in a typical fuel/moderator configuration is of the order of 10^{-11}, even for high flux reactors [8]. It follows that flight lengths between subsequent collisions are exponentially distributed (hence we will call this process *exponential flights* in the following). We assume that collisions can be either of scattering or absorption type. At each scattering collision, the flight direction changes at random, whereas at absorption events the particle disappears and the flight terminates. Each flight can be seen as a random walk in the phase space of position **r** and

direction ω in a *d*-dimensional setup.

The particle density $\Psi(\mathbf{r}, \omega, t)$ represents the probability density of finding a transported particle at position **r** having direction ω at a time t, up to an appropriate normalization factor. In many applications, the actual physical observable is the average of the density $\Psi(\mathbf{r}, \omega, t)$ over the directions ω, namely

$$\Psi(\mathbf{r}, t) = \frac{1}{\Omega_d} \int \Psi(\mathbf{r}, \omega, t) d\omega, \qquad (1)$$

where $\Omega_d = \int d\omega = 2\pi^{d/2}/\Gamma(d/2)$ is a normalization factor corresponding to the surface of the unit *d*-dimensional sphere and $\Gamma()$ is the Gamma function [10].

The aim of our work is to investigate some properties of exponential flights in a generic *d*-dimensional setup. This issue has attracted a renovated interest in recent years, in that many theoretical questions remain without an answer, despite the deceivingly simple formulation of the problem; see, e.g., [11–14]. In particular, it has been emphasized that the dimension *d* deeply affects the nature of $\Psi(\mathbf{r}, t)$ and prevents in some cases from obtaining explicit results. Here, we will mostly focus on establishing insightful relationships between space, time and the statistics of particle collisions within a given volume. A number of new results will be derived, concerning unbounded, bounded, scattering as well as absorbing domains.

This paper is structured as follows. In Sec. II we recall the mathematical formalism, introduce the physical variables and derive their inter-dependence for any *d*. Then, in Sec. III we examine the distinct cases $d = 1, 2, 3$ and 4 and provide a comparison between analytical (or asymptotic) findings and Monte Carlo simulations. The presented results will concern both the spatial and temporal evolution of the particle ensemble. Conclusions will be finally drawn in Sec. IV.

II. GENERAL SETUP

Within the natural framework of statistical mechanics, the evolution of the particle density $\Psi(\mathbf{r}, \omega, t)$ for exponential flights is governed by the linear Boltzmann
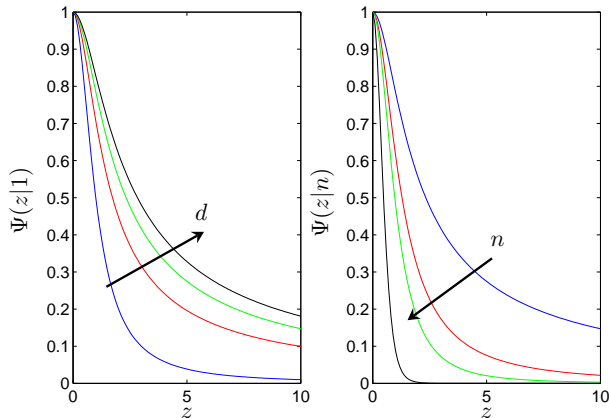
FIG. 1: The free propagator $\Psi(z|n)$ in the transformed space. Left: $\Psi(z|1)$ for increasing values of the dimension, $d = 1$ (blue), 2 (red), 3 (green), and 4 (black). Right: $\Psi(z|n)$ for $d = 3$ and increasing number of collisions, $n = 1$ (blue), 2 (red), 3 (green), and 10 (black).

equation [8]. Linearity stems from the fact of neglecting inter-particle collisions. In the hypothesis that an average particle energy can be defined (the so called one-speed transport), and that the physical properties of the medium do not depend on position nor time, the Boltzmann equation for the density $\Psi(\mathbf{r}, \omega, t)$ reads [8, 11]

$$\frac{1}{v}\frac{\partial}{\partial t}\Psi(\mathbf{r}, \omega, t) + \omega \cdot \nabla_{\mathbf{r}}\Psi(\mathbf{r}, \omega, t) =$$
$$= -\sigma_t\Psi(\mathbf{r}, \omega, t) + \sigma\int k(\omega', \omega)\Psi(\mathbf{r}, \omega', t)d\omega' + \frac{\mathcal{Q}}{v}, \quad (2)$$

where σ_t is total cross section of the traversed medium (carrying the units of an inverse length), σ is the scattering cross section, v is the particle speed, and $\mathcal{Q}$ is the source. The total cross section σ_t is such that $1/\sigma_t$ represents the average flight length between consecutive collisions (the so-called mean free path), and is related to the scattering cross section σ and to the absorption cross section σ_a by $\sigma_t = \sigma + \sigma_a$. The quantity $k(\omega', \omega)$ is the scattering kernel, i.e., the probability density that at each scattering collision the random direction changes from ω' to ω.

Denoting by $\Psi(\mathbf{r}, \omega, t)$ the solution of the Boltzmann equation (2) for a medium without absorptions ($\sigma_a = 0$), the complete solution with absorption $\Psi_a(\mathbf{r}, \omega, t)$ can be easily obtained by letting

$$\Psi_a(\mathbf{r}, \omega, t) = \Psi(\mathbf{r}, \omega, t)e^{-v\sigma_a t}, \quad (3)$$

thanks to linearity [11]. This allows primarily addressing a purely scattering medium ($\sigma_t = \sigma$), without loss of generality.

At long times, i.e., far from the source, the direction-averaged particle density $\Psi(\mathbf{r}, t)$ is known to converge to
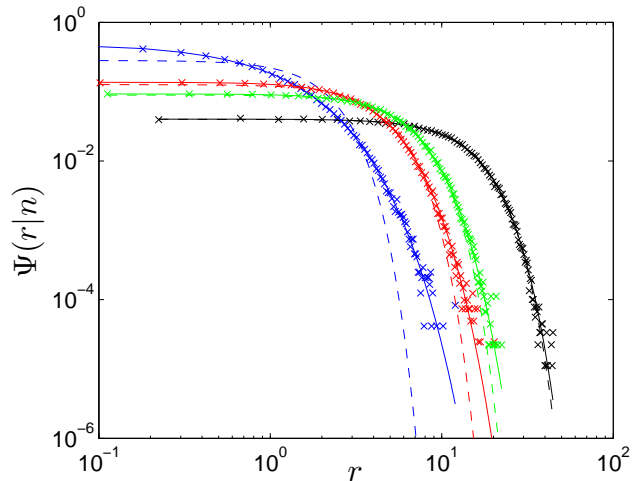

FIG. 2: The free propagator $\Psi(r|n)$ for $d = 1$, with $n = 1$ (blue), 5 (red), 10 (green), and 50 (black). Monte Carlo simulation results are displayed as symbols. The solid line is the theoretical result, Eq. (53). The dashed line is the diffusion limit, Eq. (16).

a Gaussian shape, namely,

$$\Psi(\mathbf{r}, t) \simeq \frac{e^{-\frac{|\mathbf{r}|^2}{4Dt}}}{(4\pi Dt)^{d/2}}, \quad (4)$$

the quantity $D = v/(d\sigma)$ playing the role of a diffusion coefficient [8]. However, Eq. (4) is approximately valid for $r\sigma \gg 1$, and can not capture the particle evolution at early times, nor the finite-speed propagation effects. Indeed, diffusion implicitly assumes a non-vanishing probability of finding the particles at arbitrary distance from the source.

In the following, we outline the relation between $\Psi(\mathbf{r}, t)$ and the underlying exponential flight process.

A. The free propagator without absorptions

Consider a d-dimensional setup. A particle, originally located at position $\mathbf{r}_0$ in a given domain, travels along straight lines at constant speed v, until it collides with the medium. The position of a particle at the n-th collision can be expressed as a random walk $\mathbf{r}_n = \mathbf{r}_0 + \sum_{i=1}^{n}\mathbf{r}_i$, i.e., a sum of random variables $\mathbf{r}_i$. The flight lengths $\ell = |\mathbf{r}_i - \mathbf{r}_{i-1}|$ are assumedly identically distributed and obey an exponential probability density

$$\varphi(\ell) = \sigma_t e^{-\ell\sigma_t}, \quad (5)$$

with $\sigma_t > 0$.

At each collision, the particle randomly changes its direction according to the scattering kernel $k(\omega', \omega)$. For the sake of simplicity, we assume here that the scattering is isotropic, so that $k(\omega', \omega)$ has a uniform distribution, independent of the incident direction ω'.
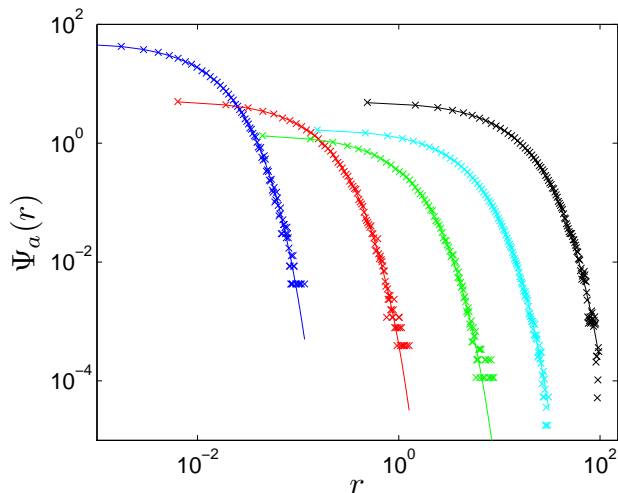
FIG. 3: The collision density with absorptions $\Psi_a(r)$ for $d = 1$, with $p = 0.01$ (blue), 0.1 (red), 0.5 (green), 0.9 (cyan), and 0.99 (black). Monte Carlo simulation results are displayed in symbols. The solid lines are the theoretical formula, Eq. (57).

FIG. 4: The collision density $\Psi(r)$ with boundaries at $r = R$ for $d = 1$, with $R = 0.5$ (blue), 1 (red), 2 (green), and 4 (black). Monte Carlo simulation results are displayed in symbols. The solid lines are the theoretical formula, Eq. (60).

Once a flight length has been sampled from $\varphi(\ell)$, the new direction ω is therefore uniformly distributed on the d-sphere of surface $\ell^{d-1}\Omega_d$. Hence, by virtue of the apparent spherical symmetry the transition kernel, i.e., the probability density of performing a displacement from $\mathbf{r}_{i-1}$ to $\mathbf{r}_i$, depends only on $\ell = |\mathbf{r}_i - \mathbf{r}_{i-1}|$, and reads

$$\pi_d(\ell) = \frac{\varphi(\ell)}{\ell^{d-1}\Omega_d}. \tag{6}$$

We initially neglect absorptions, so that $\sigma_t = \sigma$: in one-speed transport, this condition can be either seen as the particles been scattered, or equivalently being absorbed and then re-emitted (with the same speed) at each collision. This latter interpretation would correspond, e.g., to a *criticality* condition in multiplicative systems for neutron transport.

We define then the free propagator $\Psi(\mathbf{r}|n)$ as the probability density of finding a particle at position $\mathbf{r}$ at the n-th collision, for an infinite medium, i.e., in absence of boundaries. We adopt here the convention that the particle position and direction refer to the physical properties before entering the collision; for instance, the index $n = 1$ refers to uncollided particles, i.e., particles coming from the source and entering their first collision.

Assuming that all the particles are isotropically emitted at $\mathbf{r}_0 = \mathbf{0}$, the particle density $\Psi(\mathbf{r}|n)$ must depend only on the variable $r = |\mathbf{r}|$, because of the spherical symmetry. On the basis of the properties exposed above, the particle propagation as a function of the number of collisions is a Markovian process in the variable $\mathbf{r}_n$, where for each collision $i = 1, ..., n$ the new propagator is given by the convolution integral

$$\Psi(r|i) = \int \pi_d(|\mathbf{r} - \mathbf{r}'|)\Psi(r'|i-1)d\mathbf{r}', \tag{7}$$

with initial condition $\Psi(r|0) = \delta(r)$. In particular, by direct integration we immediately get the uncollided propagator

$$\Psi(r|1) = \pi_d(r). \tag{8}$$

It is convenient to introduce the d-dimensional Fourier transform of spherical-symmetrical functions, as in the subsequent analysis this will allow easier deriving of the properties of the exponential flights. Denoting by z the transformed variable with respect to r, for any spherical-symmetrical function $f(r)$ we have the following transform and anti-transform pair $f(z) = \mathcal{F}_d\{f(r)\}$ and $f(r) = \mathcal{F}_d^{-1}\{f(z)\}$ [5]

$$f(z) = z^{1-d/2}(2\pi)^{d/2}\int_0^{+\infty} r^{d/2}J_{d/2-1}(zr)f(r)dr$$

$$f(r) = r^{1-d/2}(2\pi)^{-d/2}\int_0^{+\infty} z^{d/2}J_{d/2-1}(rz)f(z)dz, \tag{9}$$

where $J_\nu()$ is the modified Bessel function of the first kind, with index ν [10]. It is apparent from Eqs. (9) that the dimension d of the system plays a fundamental role, in that it affects both the transition kernel and the Fourier transform kernel itself.

The convolution integral in Eq. (7) in Fourier space gives the algebraic relation

$$\Psi(z|i) = \pi_d(z)\Psi(z|i-1), \tag{10}$$

$i \geq 1$, with initial condition $\Psi(z|0) = 1$. By recursion, it follows that in the transformed space

$$\Psi(z|n) = \pi_d(z)^n. \tag{11}$$

FIG. 5: The free propagator $\Psi(r|n)$ for $d = 2$, with $n = 1$ (blue), 5 (red), 10 (green), and 50 (black). Monte Carlo simulation results are displayed in symbols. The solid line is the theoretical result, Eq. (65). The dashed line is the diffusion limit, Eq. (16).
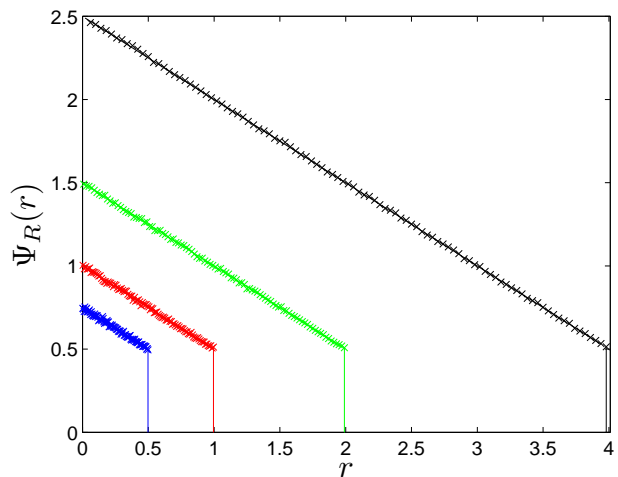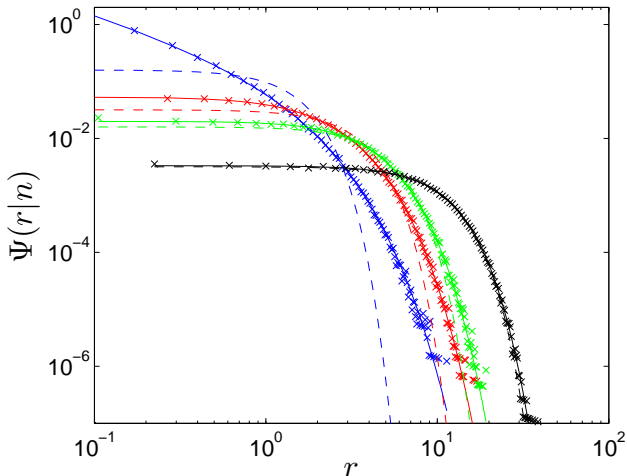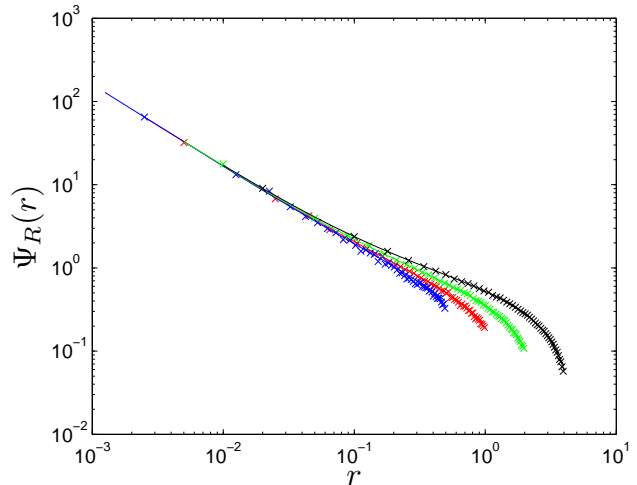

FIG. 6: The collision density $\Psi(r)$ with boundaries at $r = R$ for $d = 2$, with $R = 0.5$ (blue), 1 (red), 2 (green), and 4 (black). Monte Carlo simulation results are displayed in symbols. The solid lines are the theoretical formula in Eq. (68).

It turns out that the Fourier transform of the transition kernel $\pi_d(z)$ can be explicitly performed in arbitrary dimension, and gives

$$\pi_d(z) = {}_2F_1\left(\frac{1}{2}, 1, \frac{d}{2}; -\frac{z^2}{\sigma^2}\right), \tag{12}$$

where ${}_2F_1$ is the Gauss hypergeometric function [10]. Hence, we finally obtain

$$\Psi(z|n) = \left[{}_2F_1\left(\frac{1}{2}, 1, \frac{d}{2}; -\frac{z^2}{\sigma^2}\right)\right]^n. \tag{13}$$

The quantity $\pi_d(z)$ is positive for $d \geq 1$; moreover, $\pi_d(z = 0) = 1$, which ensures normalization and positivity of the propagator. In Fig. 1 we visually represent the effects of dimension and number of collisions on the shape of $\Psi(z|n)$. Remark in particular that the spread of $\Psi(z|n)$ increases with d, for a given n. On the contrary, $\Psi(z|n)$ becomes more peaked around the origin with growing n, for a given d.

Formally, performing the inverse Fourier transform of Eq. (13) gives the propagator $\Psi(r|n) = \mathcal{F}_d^{-1}\{\Psi(z|n)\}$ for an arbitrary d-dimensional setup. Actually, in some cases this task turns out to be non-trivial. Nonetheless, even in absence of an explicit functional form for the propagator, information can be extracted by resorting to the Tauberian theorems. In particular, the expansion of $\Psi(z|n)$ for $z/\sigma \ll 1$ gives the behavior of $\Psi(r|n)$ for $r\sigma \gg 1$, i.e., far from the source, in the so-called *diffusion limit* [3, 4]; viceversa, the expansion of $\Psi(z|n)$ for $z/\sigma \gg 1$ gives the behavior of $\Psi(r|n)$ for $r\sigma \ll 1$, i.e., close to the source. We recall that ${}_2F_1$ is defined through the series [10]

$${}_2F_1\left(\frac{1}{2}, 1, \frac{d}{2}; -\frac{z^2}{\sigma^2}\right) = \sum_{k=0}^{\infty} \frac{\Gamma\left(\frac{d}{2}\right)\Gamma\left(\frac{1}{2} + k\right)}{\sqrt{\pi}\Gamma\left(\frac{d}{2} + k\right)}\left(i\frac{z}{\sigma}\right)^{2k}. \tag{14}$$

At the leading order for $z/\sigma \to 0$ we therefore have

$$\pi_d(z) \simeq 1 - \frac{1}{d}\left(\frac{z}{\sigma}\right)^2 + ... \tag{15}$$

Observe that Eq. (15) can be viewed as the expansion of an exponential function. Then, the inverse Fourier transform gives the Gaussian shape

$$\Psi(r|n) \simeq \frac{e^{-\frac{r^2}{4n\mathcal{D}}}}{(4\pi\mathcal{D}n)^{d/2}}, \tag{16}$$

which is valid for $r\sigma \gg 1$, $\mathcal{D} = 1/(d\sigma^2)$ playing the role of a diffusion coefficient. This stems from the exponential flights having finite-variance increments, $\langle \ell^2 \rangle < +\infty$, so that their probability density $\Psi(r|n)$ falls in the basin of attraction of the Central Limit Theorem [3]. Remark the close analogy between Eqs. (4) and (16): in particular, $\mathcal{D}$ and D differ by a factor σv, which roughly speaking represents the average number of collisions per unit time.

Moreover, at the leading order for $z/\sigma \to \infty$ we have the expansion

$$\pi_d(z) \simeq \frac{\sqrt{\pi}\Gamma\left(\frac{d}{2}\right)}{\Gamma\left(\frac{d-1}{2}\right)}\left(\frac{\sigma}{z}\right) + (2 - d)\left(\frac{\sigma}{z}\right)^2 + ..., \tag{17}$$

where the first term vanishes for $d = 1$. By inverse Fourier transforming, we have for $r\sigma \ll 1$

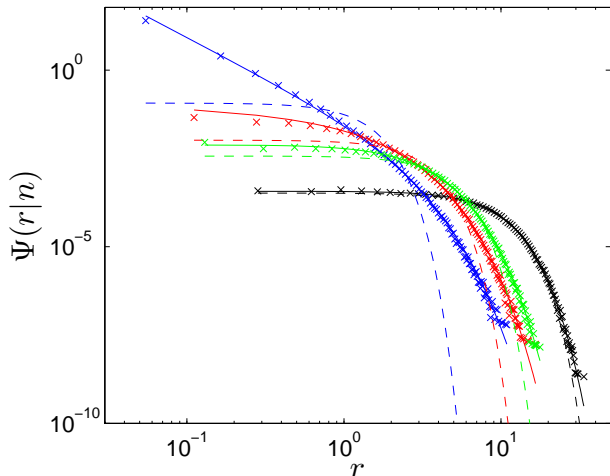$$\Psi(r|n) \simeq c_1^{n,d} + c_2^{n,d}(r\sigma)^{n-d}, \tag{18}$$

FIG. 7: The free propagator $\Psi(r|n)$ for $d = 3$, with $n = 1$ (blue), 5 (red), 10 (green), and 50 (black). Monte Carlo simulation results are displayed in symbols. The dashed line is the diffusion limit, Eq. (77). The solid line is the approximate propagator, Eq. (73).
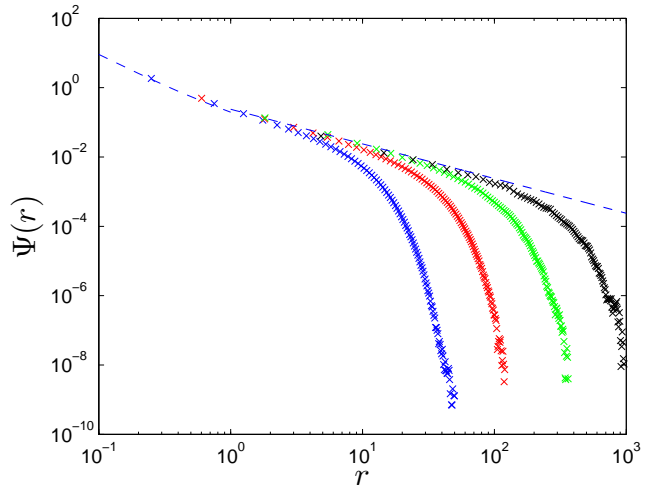

FIG. 8: The collision density $\Psi(r)$ for $d = 3$, with increasing number of summed collisions, $N = 10^2$ (blue), 10^3 (red), 10^4 (green), and 10^5 (black). The dashed lines are the asymptotic limits close (Eq. (82)) and far (Eq. (81)) from the source.

when $d > 1$, and $\Psi(r|n) \simeq c_1^{n,1} + c_2^{n,1}(r\sigma)^{2n-1}$ when $d = 1$. Here $c_1^{n,d}$ and $c_2^{n,d}$ are constants depending on n and d. It can be shown that the divergence at the origin in $\Psi(r|n)$ due to the Dirac delta source disappears after $n > d$ collisions for $d > 1$, and $n \geq 1$ for $d = 1$.

B. Relation between collision number and time

Assume again that $\sigma_t = \sigma$, i.e., that there are no absorptions. The free propagator $\Psi(r|n)$ gives information on the position of a transported particle at the moment of entering the n-th scattering collision. The link between the travelled distance, the flight time and the number of collisions is provided by the velocity v. Indeed, once a flight of length ℓ between any two collisions has been sampled from $\varphi(\ell)$, the flight time must satisfy $t_\ell = t_i - t_{i-1} = \ell/v$. Hence, the transition kernel, i.e., the probability density of performing a displacement from $\mathbf{r}_{i-1}$ at t_{i-1} to $\mathbf{r}_i$ at t_i, will be given by

$$\pi_d(\ell, t_\ell) = \pi_d(\ell)\delta\left(t_\ell - \frac{\ell}{v}\right). \qquad (19)$$

It follows that inter-collision times are exponentially distributed

$$w(t_\ell) = \int \pi_d(\ell, t_\ell)\Omega_d\ell^{d-1}d\ell = \frac{e^{-t_\ell/\tau}}{\tau}, \qquad (20)$$

where $\tau = 1/(\sigma v)$ represents the average time between collisions. Moreover, the number of collisions n each particle undergoes in a time span t obeys a Poisson distri-

bution, namely,

$$\mathcal{P}(n; t) = \frac{\left(\frac{t}{\tau}\right)^n e^{-t/\tau}}{n!}. \qquad (21)$$

We define the propagator $\Psi(r, t|n)$ as the probability density of finding a particle at position $\mathbf{r}$ at time t at the n-th collision. From the Markov property of the process, at each collision $i = 1, ..., n$ we have

$$\Psi(r, t|i) = \int d\mathbf{r}' \int dt' \pi_d(|\mathbf{r} - \mathbf{r}'|, t - t')\Psi(r', t'|i - 1), \qquad (22)$$

with initial condition $\Psi(r, t|0) = \delta(r)\delta(t/\tau) = \tau\mathcal{Q}(r, t)$. In particular, by direct integration we immediately get the uncollided propagator

$$\Psi(r, t|1) = \pi_d(r, t) = \tau\Psi(r|1)\delta\left(t - \frac{r}{v}\right). \qquad (23)$$

We denote the Laplace transform of a function $g(t)$ by its argument, i.e.,

$$g(s) = \mathcal{L}\{g(t)\} = \int_0^{+\infty} e^{-st}g(t)dt. \qquad (24)$$

Then, from the double convolution integral in Eq. (22) we have the algebraic product in the Fourier and Laplace space

$$\Psi(z, s|i) = \pi_d(z, s)\Psi(z, s|i - 1), \qquad (25)$$

$i \geq 1$, with $\Psi(z, s|0) = \tau$. By recursion, it follows that in the transformed space we have

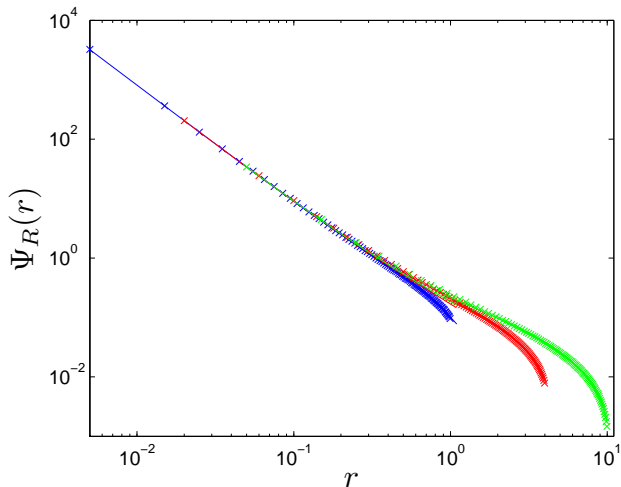$$\Psi(z, s|n) = \tau\pi_d(z, s)^n. \qquad (26)$$

FIG. 9: The collision density $\Psi(r)$ for $d = 3$, with leakages at $R = 1$ (blue), 4 (red), and 10 (green). Monte Carlo simulation results are displayed in symbols. The solid lines are the asymptotic limits close to and far from the source, as provided by the method of images.
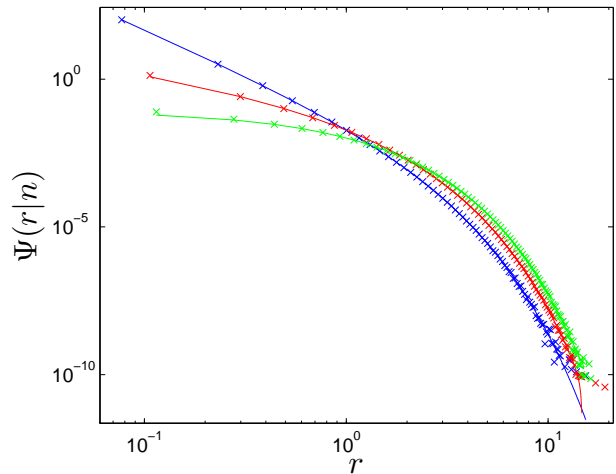

FIG. 10: The propagator $\Psi(r|n)$ for $d = 4$, with $n = 1$ (blue), 3 (red), and 5 (green). Monte Carlo simulation results are displayed in symbols. The solid lines are the theoretical formula in Eq. (91).

It turns out that the Fourier and Laplace transform of the transition kernel $\pi_d(z, s)$ can be explicitly performed in arbitrary dimension, and gives

$$\pi_d(z, s) = \frac{{}_2F_1\left(\frac{1}{2}, 1, \frac{d}{2}; -\frac{z^2}{\zeta^2}\right)}{1 + s\tau}, \tag{27}$$

where $\zeta(s) = \sigma(1 + s\tau)$. Hence, we finally obtain

$$\Psi(z, s|n) = \tau \left[\frac{{}_2F_1\left(\frac{1}{2}, 1, \frac{d}{2}; -\frac{z^2}{\zeta^2}\right)}{1 + s\tau}\right]^n. \tag{28}$$

Moreover, the following relation follows: $\Psi(z, s = 0|n) = \tau\Psi(z|n)$, so that

$$\Psi(r|n) = \frac{1}{\tau} \int_0^{+\infty} \Psi(r, t|n)dt, \tag{29}$$

i.e., $\Psi(r|n)$ can be intepreted as the time average of $\Psi(r, t|n)$. Finally, the propagator $\Psi(r, t)$ will be given by the sum of the contributions $\Psi(r, t|n)$ at each collision, namely

$$\Psi(r, t) = \sum_{n=1}^{\infty} \Psi(r, t|n). \tag{30}$$

Taking the Fourier and Laplace transform of Eq. (30), we then have

$$\Psi(z, s) = \sum_{n=1}^{\infty} \Psi(z, s|n) = \tau \frac{\pi_d(z, s)}{1 - \pi_d(z, s)}, \tag{31}$$

with $\Psi(r, t) = \mathcal{L}^{-1}\mathcal{F}_d^{-1}\{\Psi(z, s)\}$.

C. Absorptions

In presence of absorptions ($\sigma_a > 0$), the propagator $\Psi_a(r, t)$ can be obtained from Eq. (3) by integrating over directions. This relation holds true at each collision, so that we have

$$\Psi_a(r, t|n) = \Psi(r, t|n)e^{-t/\tau_a}, \tag{32}$$

where $\tau_a = 1/(\sigma_a v)$. Hence, from Eq. (29), by replacing σ with σ_t we get for the propagator $\Psi_a(z|n)$

$$\Psi_a(z|n) = \frac{1}{\tau_t} \int_0^{+\infty} \Psi_a(z, t|n)dt = \frac{1}{\tau_t}\Psi(z, s = \frac{1}{\tau_a}|n), \tag{33}$$

where $\tau_t = 1/(\sigma_t v)$ represents the average flight time between any two collisions. Now, observe that from Eq. (28) we have

$$\Psi\left(z, s = \frac{1}{\tau_a}|n\right) = \tau\Psi\left(z\frac{\sigma}{\sigma_t}|n\right)\left(\frac{\sigma}{\sigma_t}\right)^n, \tag{34}$$

where the quantity $p = \sigma/\sigma_t$, $0 < p < 1$, can be interpreted as the the probability of being scattered, i.e., *not* being absorbed, at any given collision. Then, by remarking that $\tau/\tau_t = 1/p$, it follows that

$$\Psi_a(z|n) = \Psi(pz|n)p^{n-1}. \tag{35}$$

The propagator in Eq. (35) is then given by the product of the free propagator, with the total cross section σ_t replacing the scattering cross section σ, times the probability of having survived up to entering the n-th collision. Remark that the total cross section and the non-absorption probability are related by $\sigma = p\sigma_t$. When the absorption length is infinite, $\sigma_a \to 0$, $p \to 1$ and we recover the free propagator for pure scattering, with $\sigma_t = \sigma$.
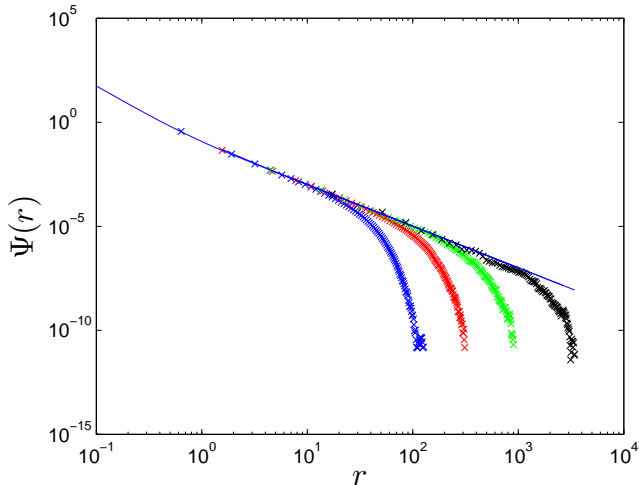
FIG. 11: The collision density $\Psi(r)$ for $d = 4$, with increasing number of summed collisions, $N = 10^2$ (blue), 10^3 (red), 10^4 (green), and 10^5 (black). The solid lines are the theoretical formula in Eq. (94).
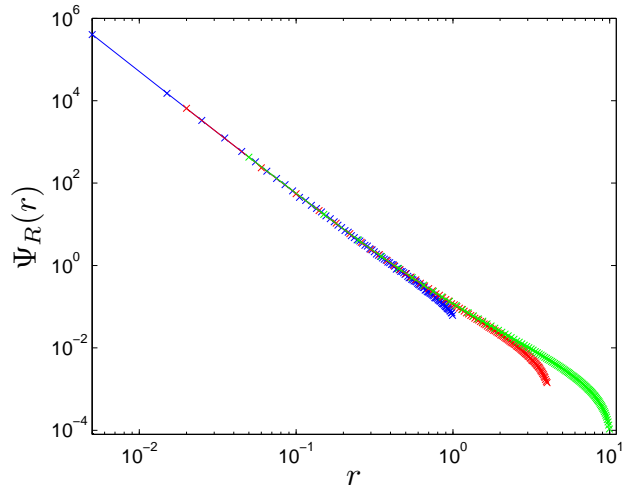

FIG. 12: The collision density $\Psi(r)$ for $d = 4$, with leakages at $R = 1$ (blue), 4 (red), and 10 (green). Monte Carlo simulation results are displayed in symbols. The solid lines are the theoretical results from the method of images.

D. Boundary conditions

So far, we have assumed that the medium where particles are transported has an infinite extension, hence the name free propagator. More realistically, we might consider finite-extension media with volume $\mathcal{V}$ enclosing the source, so that boundary conditions come into play and affect the nature of the propagator. Several boundary conditions can be conceived according to the specific physical system, among which the most common are reflecting and leakage. Here we will focus on leakage boundary conditions, where particles are considered lost as soon as their trajectory has traversed the outer boundary $\partial\mathcal{V}$ of the domain. While the volume $\mathcal{V}$ is in principle totally arbitrary, in the subsequent calculations for the sake of convenience we will assume that $\mathcal{V} = \mathcal{V}(R)$ is a sphere of radius R centered in $\mathbf{r_0} = \mathbf{0}$.

From the point of view of the propagator, leakages can be taken into account by assuming that the population density $\Psi(r|n)$ at any n vanishes at the so-called extrapolation length r_e, i.e., $\Psi(r = r_e|n) = 0$ [6–8]. Because trajectory do not terminate at the boundary, but rather at the first collision occurred outside the volume, the extrapolation length is expected to be larger than the physical boundary of $\mathcal{V}(R)$ and can be determined from solving the so-called Milne's problem associated to the volume [16, 17]. In general, r_e is of the kind $r_e = R[1 + u_d/(R\sigma)]$, the dimensionless constant $u_d > 0$ depending on the dimension of the system [16]. When the scattering length is much smaller than the typical size of the volume, i.e., $\sigma R \gg 1$, the extrapolation length coincides with the physical boundary, $r_e \to R$. This means that the inter-collision length is so small as compared to the total travelled distance that the first collision out-

side the domain will actually be very close to the last collision inside the domain, which corresponds to $\Psi(r|n)$ vanishing at R [3, 8].

E. Spatial moments of the propagator

The moments of the propagator provide an estimate of the spatial evolution of the particles ensemble, as a function of the number of collisions or time. Due to the supposed spherical symmetry, we expect all the odd moments to vanish. We define the m-th moment of $f(r)$ over the spherical shell $r^{d-1}\Omega_d dr$ as

$$\langle r^m \rangle = \Omega_d \int_0^{+\infty} r^{m+d-1} f(r) dr. \qquad (36)$$

Performing the integral in Eq. (36) would require explicitly knowing $f(r)$. However, as shown in the Appendix A, the m-th spatial moment $f(r)$ of can be expressed as a function of the m-th derivative of $f(z)$ with respect to z

$$\langle r^m \rangle = \frac{\sqrt{\pi}\Gamma\left(\frac{d+m}{2}\right)}{\Gamma\left(\frac{d}{2}\right)\Gamma\left(\frac{1+m}{2}\right)} \frac{\partial^m}{\partial(iz)^m} [f(z)]_{z=0} \qquad (37)$$

when m is even, and $\langle r^m \rangle = 0$ otherwise. By setting $f(z) = \Psi(pz|n)p^{n-1}$ in Eq. (37) we then have $\langle r^m \rangle(n)$ as a function of the number of collisions. Analogously, by setting $f(z) = \Psi_a(z, s) = \Psi(z, s + 1/\tau_a)$ we get $\langle r^m \rangle(s)$, which gives the evolution as a function of time, upon inverse Laplace transforming. In particular, for the spread $m = 2$ of the propagator with absorptions we get

$$\langle r^2 \rangle(n) = \frac{2}{\sigma_t^2} p^{n-1} n, \qquad (38)$$

and

$$\langle r^2 \rangle(t) = \frac{2}{\sigma^2}\left[e^{-t/\tau} - 1 + \frac{t}{\tau}\right]e^{-t/\tau_a}. \qquad (39)$$

In absence of absorptions, $\tau_a \to \infty$ and $p \to 1$, the particle spread $\langle r^2 \rangle(n)$ is linear with respect to n. On the contrary, $\langle r^2 \rangle(t)$ has a ballistic behavior ($\propto t^2$) at earlier times (where transport is dominated by velocity), and a diffusive behavior ($\propto t$) at later times (where transport is dominated by scattering). The transition between the two regimes is imposed by the time scale τ. A remarkable feature is that in either case the spread does not explicitly depend on the dimension d. Intuitively, this can be understood by considering that (independently of the dimension d of the embedding setup) the vectors $\mathbf{r}_i$ and $\mathbf{r}_{i+1}$ define a plane with random orientation, so that space is explored by plane surfaces at each collision. This is in analogy, e.g., with the beahvior of d-dimensional Brownian Motion [3].

F. Collision density

In many physical problems, one is interested in assessing the statistics of the time $t_\mathcal{V}$ or the collision number $n_\mathcal{V}$ spent inside a given domain $\mathcal{V}$. In Reactor Physics, for instance, the average number of neutron collisions within a region would be related to such issues as the nuclear heating or nuclear damage in fissile as well as structural materials [6, 7]. We introduce the collision density $\Psi(r)$, which is defined as

$$\Psi(r) = \lim_{N \to \infty}\sum_{n=1}^{N}\Psi(r|n). \qquad (40)$$

From Eq. (30), it follows that $\Psi(r)$ can be equivalently obtained from the propagator $\Psi(r,t)$ as

$$\Psi(r) = \lim_{T \to \infty}\frac{1}{\tau}\int_0^T \Psi(r,t)dt. \qquad (41)$$

For an infinite 'observation time' T, the m-th moments of the residence time $t_\mathcal{V}$ within $\mathcal{V}$ can be expressed in terms of the collision density $\Psi(r)$ in the same domain by slightly adapting an argument due to Kac [18]

$$\frac{\langle t_\mathcal{V}^m \rangle}{\tau^m} = m!\int_\mathcal{V} d\mathbf{r}_m ... \int_\mathcal{V} d\mathbf{r}_1 \Psi(r_m)...\Psi(r_1), \qquad (42)$$

where $r_i = |\mathbf{r}_i - \mathbf{r}_{i-1}|$. From Eq. (42) it is then apparent that performing repeated integrals of the collision density $\Psi(r)$ allows computing all the moments $\langle t_\mathcal{V}^m \rangle$, which in turn allows reconstructing the full distribution $\mathcal{Q}(t_\mathcal{V})$ of the residence time within the domain.

Moreover, by virtue of the counting statistics of Eq. (21), we are able to characterize the moments of the collision number $n_\mathcal{V}$ within $\mathcal{V}$ in terms of the associated $\langle t_\mathcal{V}^m \rangle$. Indeed, we have

$$\langle n_\mathcal{V}^m \rangle_{t_\mathcal{V}} = \sum_{n=1}^{+\infty} n^m \mathcal{P}(n; t_\mathcal{V}), \qquad (43)$$

which depends on the stochastic realizations of the residence times $t_\mathcal{V}$. Now, by taking the average of $\langle n_\mathcal{V}^m \rangle_{t_\mathcal{V}}$ with respect to $\mathcal{Q}(t_\mathcal{V})$, we obtain

$$\langle n_\mathcal{V}^m \rangle = \langle\langle n_\mathcal{V}^m \rangle_{t_\mathcal{V}}\rangle = \langle \mathcal{B}_m\left[\frac{t_\mathcal{V}}{\tau}\right]\rangle. \qquad (44)$$

Here $\mathcal{B}_m[x] = \sum_{k=1}^m S_{m,k}x^k$ are Bell polynomials, whose coefficients are given by the Stirling numbers of second kind

$$S_{m,k} = \frac{1}{k!}\sum_{i=0}^k (-1)^i\binom{k}{i}(k-i)^m. \qquad (45)$$

These quantities commonly arise in computing the moments of Poisson distributions [10]. Thanks to linearity, Eq. (44) allows expressing $\langle n_\mathcal{V}^m \rangle$ as a combination of m moments $\langle t_\mathcal{V}^k \rangle$, $k = 1,...,m$, each given from Eq. (42).

In particular, since $S_{1,1} = 1$, we have that

$$\langle n_\mathcal{V}^1 \rangle = \frac{\langle t_\mathcal{V} \rangle}{\tau} = \int_\mathcal{V} d\mathbf{r}_1 \Psi(r_1), \qquad (46)$$

i.e., the integral of the collision density over a volume $\mathcal{V}$ gives the mean number of collisions within that domain, hence the name given to $\Psi(r)$. Furthermore, $S_{2,1} = S_{2,2} = 1$, so that

$$\langle n_\mathcal{V}^2 \rangle = \frac{\langle t_\mathcal{V}^2 \rangle}{\tau^2} + \frac{\langle t_\mathcal{V} \rangle}{\tau} = \int_\mathcal{V} d\mathbf{r}_2 \int_\mathcal{V} d\mathbf{r}_1 \Psi(r_2)\Psi(r_1) + \langle n_\mathcal{V}^1 \rangle. \qquad (47)$$

Remark that both $\langle t_\mathcal{V}^m \rangle$ and $\langle n_\mathcal{V}^m \rangle$ depend on the boundary conditions imposed on $\partial\mathcal{V}$, which in turn affect the functional form of the propagator, and then $\Psi(r)$. Using a free propagator corresponds to defining a fictitious volume $\mathcal{V}$, whose boundaries $\partial\mathcal{V}$ are 'transparent', so that particles can indefinitely cross $\partial\mathcal{V}$ back an forth. On the contrary, the use of leakage boundary conditions leads to the formulation of first-passage problems, i.e., determining the distribution of the time, or collision number, required to first reach the boundary [15].

The previous discussion shows that $\Psi(r)$ is key in determining residence times and collisions statistics. After formally carrying out the summation in Eq. (40), we have $\Psi(z) = \pi_d(z)/[1 - \pi_d(z)]$, so that $\Psi(r)$ for a free propagator in absence of absorptions is defined in terms of the following Fourier integral

$$\Psi(r) = \frac{r^{1-d/2}}{(2\pi)^{d/2}}\int_0^{+\infty} z^{d/2}J_{d/2-1}(rz)\frac{\pi_d(z)}{1-\pi_d(z)}dz, \qquad (48)$$

whose convergence depends on the dimension d of the system. It turns out that convergence is ensured for $d > 2$,

which means that for $1d$ and $2d$ finite-size domains with transparent boundaries $\langle n_{\mathcal{V}}^1 \rangle$ and $\langle t_{\mathcal{V}}^1 \rangle$ diverge as $N \to \infty$. This result is in analogy with Pólya's theorem, which states that random walks on Euclidean lattices are recurrent for $d \le 2$ [3]. As shown in the following, we can nonetheless provide an estimate of such divergence as a function of N, i.e., single out a singular term from a functional form. For finite domains with leakage boundary conditions and/or absorptions ($\sigma_a > 0$), $\Psi(r)$ is defined also for $1d$ and $2d$ systems. For $d > 2$, Tauberian theorems show that the asymptotic behavior of Eq. 48 is given by

$$\Psi(r) \simeq \frac{\Gamma\left(\frac{d}{2}\right)}{2\pi^{d/2}}(r\sigma)^{2-d} \qquad (49)$$

for large r, and

$$\Psi(r) \simeq \frac{\Gamma\left(\frac{d}{2}\right)}{2\pi^{d/2}}(r\sigma)^{1-d} \qquad (50)$$

close to the source.

III. ANALYSIS OF d-DIMENSIONAL SETUPS

In the following, we detail the results pertaining to specific values of d. We choose $1/\sigma_t$ as length scale and we work with dimensionless spatial variables $r = r\sigma_t$. Remark that in absence of absorptions the length scale is $1/\sigma$, since $p = 1$.

A. One-dimensional setup, $d = 1$

The case $d = 1$ allows illustrating the general structure of the calculations. The transition kernel is

$$\pi_1(\ell) = \frac{e^{-\ell}}{2}, \qquad (51)$$

whose Fourier transform is

$$\pi_1(z) = \frac{1}{1 + z^2}. \qquad (52)$$

Starting from $\Psi(z, 0) = 1$, the free propagator $\Psi(r|n)$ can be explicitly obtained by performing the inverse Fourier transform of $\Psi(z|n) = \pi_1(z)^n$, and reads

$$\Psi(r|n) = \frac{2^{\frac{1}{2}-n}r^{-\frac{1}{2}+n}K_{-\frac{1}{2}+n}(r)}{\sqrt{\pi}\Gamma(n)}, \qquad (53)$$

where $K_\nu()$ is the modified Bessel function of the second kind, with index ν [10]. The same formula has been recently derived, e.g., in [14] as a particular case of a broader class of random flights. In Fig. 2 we provide a comparison between Monte Carlo simulation results (symbols), the analytical formula Eq. (53) (solid lines), and the diffusion limit, Eq. (16) (dashed lines),

for different values of n. Remark in particular that the diffusion limit is not accurate for small n, and becomes progressively closer to the exact result for increasing n, as expected. At intermediate n, the tails of the propagator (53) are always fatter than those predicted by the diffusion approximation.

In a $1d$ setup, the collision density $\Psi(r)$ for the free propagator diverges. Nonetheless, it is possible to single out the divergence as follows

$$\Psi(z) = \lim_{N \to \infty} \sum_{n=1}^{N} \Psi(z|n) = \lim_{N \to \infty} \frac{1 - \left(1 + z^2\right)^{-N}}{z^2}. \qquad (54)$$

For fixed N, the inverse transform can be explicitly performed in terms of hypergeometric functions. Retaining the non-vanishing terms for large N, we have

$$\Psi(r) \simeq \frac{\Gamma\left(\frac{1}{2} + N\right)}{\Gamma(N)\sqrt{\pi}} - \frac{r}{2} \simeq \frac{\sqrt{N}}{\sqrt{\pi}} - \frac{r}{2}, \qquad (55)$$

which is composed of a term diverging with $\sqrt{N}$ (not depending on r), and a functional part which is linear in r (not depending on N).

For the propagator with absorptions, from Eq. (35) we have

$$\Psi_a(z) = \lim_{N \to \infty} \sum_{n=1}^{N} \Psi(z|n)\, p^{n-1} = \frac{1}{1 - p + z^2}. \qquad (56)$$

Then, performing the inverse Fourier transform, we get

$$\Psi_a(r) = \frac{e^{-\sqrt{1-p}\,r}}{2\sqrt{1-p}}. \qquad (57)$$

Remark that Eq. (57) has been derived, e.g., in [19] by solving the stationary Boltzmann equation in $1d$. In Fig. 3 we compare Monte Carlo simulation results (symbols) with Eq. (57) (solid line). When $p \to 0$, the particles are almost surely absorbed at the first collision, and we have the expansion

$$\Psi_a(r) \simeq \frac{e^{-r}}{2}\left(1 + \frac{p}{2} + \frac{pr}{2}\right) + ..., \qquad (58)$$

so that at the first order the collision density has the same functional form as the uncollided propagator. At the opposite, when $p \to 1$ the particles are almost surely always scattered ($\sigma_t \to \sigma$), and we have the expansion

$$\Psi_a(r) \simeq \frac{1}{2\sqrt{1-p}} - \frac{r}{2} + ..., \qquad (59)$$

and $\Psi_a(r)$ diverges as the collision density associated to the free propagator, as expected.

The case of leakage boundary conditions can be dealt with by imposing that the propagator $\Psi(r|n)$ must vanish for any n at the extrapolated boundary r_e. For $d = 1$, the extrapolated length is given by $r_e = R[1 + u_d/R]$ with $u_1 = 1$ [16], i.e., the propagator must vanish at one

scattering length outside the physical border R of the domain. By resorting to the method of images [3], which allows solving for the propagator in presence of boundaries in terms of the propagator in absence of boundaries, we therefore have for the collision density

$$\Psi_R(r) = \frac{r_e - r}{2}, \qquad (60)$$

for $r \leq R$, and $\Psi(r) = 0$ elsewhere. In Fig. 4 we compare the Monte Carlo simulation results with the theoretical formula in Eq. (60).

The moments of the number of collisions within a sphere of radius R can be explicitly computed based on Eq. (44). The moments associated to the free propagator clearly diverge. Here we separately analyze the propagator with absorption (in an infinite domain) and the propagator with leakages at the boundary $r = r_e \geq R$ (without absorptions). For the case of absorptions, the average number of collisions within a (fictitious) sphere of radius R reads

$$\langle n_R^1 \rangle = \frac{1 - e^{-\sqrt{1-p}R}}{1 - p}, \qquad (61)$$

assuming that particles can cross the boundaries of the sphere an infinite number of times. When the radius of the sphere is large as compared to the typical particle displacement, we have $\langle n_R^1 \rangle \simeq 1/(1 - p)$, which gives $\langle n_R^1 \rangle \simeq 1$ when $p \to 0$, and diverges for $p \to 1$. For the case of leakages, the average number of collisions reads

$$\langle n_R^1 \rangle = \frac{R(2r_e - R)}{2}. \qquad (62)$$

When the radius of the sphere is large as compared to the typical particle displacement, $r_e \to R$, and we have $\langle n_R^1 \rangle \simeq R^2/2$.

B. Two-dimensional setup, $d = 2$

The case $d = 2$ has a key interest in assessing, e.g., the dynamics of chemical and biological species on surfaces [9]. The transition kernel reads

$$\pi_2(\ell) = \frac{e^{-\ell}}{2\pi\ell}, \qquad (63)$$

whose Fourier transform is

$$\pi_2(z) = \frac{1}{\sqrt{1 + z^2}}. \qquad (64)$$

Starting from $\Psi(z, 0) = 1$, the free propagator $\Psi(r|n)$ can be explicitly obtained by performing the inverse Fourier transform of $\Psi(z|n) = \pi_2(z)^n$, and reads

$$\Psi(r|n) = \frac{2^{-\frac{n}{2}} r^{-1 + \frac{n}{2}} K_{-1 + \frac{n}{2}}(r)}{\pi \Gamma\left(\frac{n}{2}\right)}. \qquad (65)$$

This result was previously established by [21], and more recently has appeared, e.g., in [14, 22]. In Fig. 5 we compare the Monte Carlo simulation results (symbols) with the theoretical formula in Eq. 65, for different values of n. The diffusion limit, Eq. 16 is also shown in dashed lines. Remark that the diffusion limit is not accurate for small n, and becomes progressively closer to the exact result for increasing n. At intermediate n, the tails of the propagator (65) are always fatter than those predicted by the diffusion approximation.

In a $2d$ setup, the collision density $\Psi(r)$ diverges. Nonetheless, analogously as done for the $1d$ case, it is possible to single out the divergence as follows

$$\Psi(z) = \lim_{N \to \infty} \sum_{n=1}^{N} \Psi(z|n) = \lim_{N \to \infty} \frac{1 - \left(1 + z^2\right)^{-N/2}}{\sqrt{1 + z^2} - 1}. \qquad (66)$$

For fixed N, the inverse transform can be explicitly performed. Details of the rather cumbersome calculations are left to the Appendix B. Retaining the non-vanishing terms for large N, we have

$$\Psi(r) \simeq \frac{\log(N)}{2\pi} + \frac{e^{-r}}{2\pi r} + \frac{\text{E}i(-r) - 2\log(r)}{2\pi}, \qquad (67)$$

where $\text{E}i$ is the exponential integral function [10]. To the authors' best knowledge, the formula for the collision density $\Psi(r)$ has not appeared before, and might then provide a useful tool for describing the migration of species on $2d$ environments. Similarly as in the $1d$ case, $\Psi(r)$ is composed of a term diverging with $\log N$ (not depending on r), and a functional part in r (not depending on N). In deriving Eq. (67) we have neglected a constant term which is small compared to $\log(N)$, namely, $[\log(2) - \gamma/2]/\pi$, where $\gamma \simeq 0.57721$ is the Euler's gamma constant [10].

The collision density with leakages at $r = r_e$ can be obtained again by the method of images, whence

$$\Psi_R(r) = \frac{e^{-r}}{2\pi r} - \frac{e^{-r_e}}{2\pi r_e} + \frac{\text{E}i(-r) - \text{E}i(-r_e) - 2\log\left(\frac{r}{r_e}\right)}{2\pi}, \qquad (68)$$

where $r_e = R[1 + u_2/R]$ and the Milne's constant $u_2 \simeq 1 - 2/\pi^2$ [16].

The moments associated to the free propagator clearly diverge. For the propagator with leakages at the boundary $r = r_e \geq R$ the average number of collisions within a sphere of radius R reads

$$\langle n_R^1 \rangle = \frac{1 - e^{-R} + Re^{-R} + R^2 - \frac{R^2 e^{-r_e}}{r_e}}{2} +$$
$$+ \frac{R^2 \text{E}i(-R) - R^2 \text{E}i(-r_e) - 2R^2 \log(\frac{R}{r_e})}{2}. \qquad (69)$$

When $R \gg 1$, we have $r_e \simeq R$, and we get $\langle n_R^1 \rangle \simeq (1 + R^2)/2$ in the diffusion limit.

As for the collision density with absorptions, calculations analogous to the 1d case lead to

$$\Psi_a(r) = \frac{pK_0\left(r\sqrt{1-p^2}\right)}{\pi} + \frac{1}{2\pi}\int_0^{+\infty}\frac{zJ_0\left(rz\right)}{\sqrt{1+z^2}+p}dz. \tag{70}$$

We could not find an explicit expression for the latter integral in terms of elementary functions. However, the limits for small and large scattering probability can be easily obtained, and read

$$\Psi_a(r) \simeq \frac{e^{-r}}{2\pi r} + \frac{pK_0\left(r\right)}{\pi}, \tag{71}$$

when $p \to 0$, and

$$\Psi_a(r) \simeq \frac{\log\left(\frac{1}{1-p}\right)}{2\pi} + \frac{e^{-r}}{2\pi r} + \frac{\mathrm{E}i\left(-r\right)-2\log(r)}{2\pi}, \tag{72}$$

when $p \to 1$, respectively. The former expression gives the uncollided propagator at the leading order, whereas the latter diverges logarithmically as $p \to 1$.

C. Three-dimensional setup, $d = 3$

The case $d = 3$ plays a prominent role, among others, in Reactor Physics, in that it concerns the transport of neutrons and photons through matter [6–8]. On the basis of the strikingly similar form of Eqs. (53) and (65), it would be tempting to postulate an analogous expression for the propagator in $3d$. For $d = 1$ we have indeed the functional form $\Psi(r|n) \propto r^{-1/2+n}K_{-1/2+n}(r)$, and for $d = 2$ $\Psi(r|n) \propto r^{-1+n/2}K_{-1+n/2}(r)$. Then we could conjecture an exponent $-d/2+n/d$, so that

$$\Psi^*(r|n) = \frac{r^{-1/2+n}K_{-1/2+n}(r)}{2^{\frac{1}{2}+\frac{n}{3}}\pi^{\frac{3}{2}}\Gamma\left(\frac{n}{3}\right)}, \tag{73}$$

by imposing normalization. Unfortunately, this is not the case, and $\Psi^*(r|n)$ is not the true $3d$ propagator. Actually, few explicit results can be derived, and much of the analysis is therefore devoted to the asymptotic behavior. The transition kernel reads

$$\pi_3(\ell) = \frac{e^{-\ell}}{4\pi\ell^2}, \tag{74}$$

whose Fourier transform is

$$\pi_3(z) = \frac{\arctan\left(z\right)}{z}. \tag{75}$$

The propagator $\Psi(r|n)$ with initial condition $\Psi(z,0) = 1$ involves then the following integral

$$\Psi(r|n) = \frac{1}{2\pi^2 r}\int_0^{+\infty} z\sin\left(rz\right)\left[\frac{\arctan\left(z\right)}{z}\right]^n dz, \tag{76}$$

which can not be carried out explicitly for arbitrary n. In the diffusion limit $z \ll 1$ we have $[\arctan(z)/z]^n \simeq 1 - nz^2/3$, so that

$$\Psi(r|n) \simeq \frac{3\sqrt{3}e^{-\frac{3r^2}{4n}}}{8n^{3/2}\pi^{3/2}}, \tag{77}$$

as expected from Eq. (16). In Fig. 7 we compare the Monte Carlo simulation results (symbols) with the diffusion limit, Eq. (77) (dashed lines), and with the approximate propagator, Eq. (73) (solid lines). Remark that Eq. (73) provides a fairly accurate approximation of the simulation results, except close to the source.

After carrying out the sum over n, the collision density $\Psi(r)$ is given by the following integral

$$\Psi(r) = \frac{1}{2\pi^2 r}\int_0^{+\infty} z\sin\left(rz\right)\frac{\arctan\left(z\right)}{z-\arctan\left(z\right)}dz, \tag{78}$$

which again can not be performed explicitly. As before, we consider then the asymptotic behavior. Denoting $h(z) = \arctan(z)/[z-\arctan(z)]$, we have

$$h(z) \simeq \frac{3}{z^2} + \frac{4}{5} - \frac{36}{175}z^2 + ... \tag{79}$$

in the diffusion limit $z \ll 1$, and

$$h(z) \simeq \frac{\pi}{2z} + \left(\frac{\pi^2-4}{4z^2}\right) + \left(\frac{\pi^3-8\pi}{8z^3}\right) + ... \tag{80}$$

close to the source. Similar expansions appear, e.g., in [20], as derived from the analysis of the Boltzmann equation. Correspondingly, by performing the respective integrations we have

$$\Psi(r) \simeq \frac{3}{4\pi r} \tag{81}$$

for $r \gg 1$, i.e., far from the source, and

$$\Psi(r) \simeq \frac{1}{4\pi r^2} + \left(\frac{\pi^2-4}{16\pi r}\right) + \left(\frac{8-\pi^2}{16\pi}\right)\left[\log\left(r\right)+\gamma-1\right]+... \tag{82}$$

for $r \ll 1$, i.e., close to the source. Remark that for $d = 3$ $\Psi(r)$ does not diverge even for infinite domains without absorptions. In Fig. 8 we compare the Monte Carlo simulation results (symbols) with the asymptotic limits close to and far from the source, Eqs. (82) and (81), respectively (dashed lines). The simulation results progressively approach the asymptotic limits as the number N of summed collisions increases.

Eqs. (82) and (81) can provide asymptotic estimates for the collision density with leakages at the boundary $r = R$. By the method of images, we have that the collision density with boundaries is $\Psi_R(r) = \Psi(r) - \Psi(r_e)$, with $r_e = R\left[1 + u_3/R\right]$ and $u_3 \simeq 0.7104$ [17]. In Fig. 9 we compare the Monte Carlo simulation results (symbols) with the prediction of the method of images (solid lines): an excellent agreement is found.

The moments of the number of collisions within a sphere of radius R can be explicitly computed based on Eq. (44) for the free propagator $\Psi(r|n)$, i.e., when particles can freely cross the surface of the sphere. We have

$$\langle n_R^1 \rangle \simeq \frac{3}{2} R^2 \tag{83}$$

when $R \gg 1$, and

$$\langle n_R^1 \rangle \simeq R + \frac{\pi^2 - 4}{8} R^2 \tag{84}$$

for $R \ll 1$. Moreover, for leakage boundary conditions at the surface, from $\Psi_R(r|n)$ we have

$$\langle n_R^1 \rangle \simeq \frac{R^2}{r_e} \left(\frac{3}{2} r_e - R \right) \tag{85}$$

when $R \gg 1$, and

$$\langle n_R^1 \rangle \simeq R + R^2 \frac{\pi^2 - 4}{8} + \frac{R^2}{r_e^2} \frac{r_e(4 - \pi^2) - 4}{12} \tag{86}$$

for $R \ll 1$.

D. Four-dimensional setup, $d = 4$

The case $d = 4$ is briefly presented here for the sake of completeness. The transition kernel reads

$$\pi_4(\ell) = \frac{e^{-\ell}}{2\pi^2 \ell^3}, \tag{87}$$

whose Fourier transform is

$$\pi_4(z) = \frac{2}{1 + \sqrt{1 + z^2}}. \tag{88}$$

We could not find an explicit representation for the inverse Fourier transform of $\Psi(z|n) = \pi_4(z)^n$. Nonetheless, the propagator $\Psi(r, t|n)$ is known and reads

$$\Psi(r, t|n) = \frac{n}{\Gamma(n-1)} \frac{e^{-vt}}{\pi^2(vt)^{1+n}} \left[(vt)^2 - r^2 \right]^{n-2} \tag{89}$$

for $vt \geq r$ [11]. Hence, it follows that the propagator $\Psi(r|n) = \int \Psi(r, t|n) dt/\tau$ can be obtained from solving the integral

$$\Psi(r|n) = \frac{n}{\pi^2 \Gamma(n-1)} \int_r^{+\infty} e^{-z} z^{-1-n} \left(z^2 - r^2 \right)^{n-2} dz. \tag{90}$$

This integral can be performed, and gives

$$\Psi(r|n) = \frac{1}{2^4 \pi^{3/2}} [A + B + C], \tag{91}$$

where

$$A = -n2^n \frac{\Gamma(2-n)}{\Gamma\left(\frac{5-n}{2}\right)\Gamma\left(\frac{6-n}{2}\right)} \, _1F_2 \left(2 - n, \frac{5-n}{2}, \frac{6-n}{2}; \frac{r^2}{4} \right),$$

$$B = -2^4 r^{n-4} \frac{\Gamma\left(\frac{2-n}{2}\right)}{\Gamma\left(\frac{1}{2}\right)\Gamma\left(\frac{-2+n}{2}\right)} \, _1F_2 \left(-\frac{n}{2}, \frac{1}{2}, \frac{-2+n}{2}; \frac{r^2}{4} \right),$$

$$C = 2^2 n r^{n-3} \frac{\Gamma\left(\frac{1-n}{2}\right)}{\Gamma\left(\frac{3}{2}\right)\Gamma\left(\frac{n-1}{2}\right)} \, _1F_2 \left(\frac{1-n}{2}, \frac{3}{2}, \frac{-1+n}{2}; \frac{r^2}{4} \right), \tag{92}$$

$_1F_2()$ being an hypergeometric function [10]. In Fig. 10 we compare the Monte Carlo simulation results (symbols) with the formula in Eq. (91) (solid lines).

As for the collision density $\Psi(r)$, we have

$$\Psi(r) = \frac{1}{2\pi^2 r} \int_0^{+\infty} J_1(rz) \left(1 + \sqrt{1 + z^2} \right) dz, \tag{93}$$

which can be computed explicitly and gives

$$\Psi(r) = \frac{e^{-r}}{2\pi^2 r^3} + \frac{1}{\pi^2 r^2}. \tag{94}$$

In Fig. 11 we provide a comparison between Monte Carlo simulation results (symbols) and the theoretical formula in Eq. (94) (solid line). The simulation results progressively approach the functional form of Eq. (94) as the number N of summed collisions increases.

Finally, the collision density in presence of leakages at the boundary $r = R$ can be obtained by resorting to the method of images, whence $\Psi_R(r) = \Psi(r) - \Psi(r_e)$, with $r_e = R[1 + u_4/R]$. The constant u_4 has been estimated by running a Monte Carlo simulation and determining the extrapolation length, and reads $u_4 \simeq 0.5$. In Fig. 12 we compare the Monte Carlo simulation results (symbols) and the prediction of the method of images (solid lines). An excellent agreement is found.

The moments of the number of collisions within a sphere of radius R can be explicitly computed based on Eq. (44) for the free propagator $\Psi(r|n)$, namely,

$$\langle n_R^1 \rangle = 1 + R^2 - e^{-R}. \tag{95}$$

Moreover, for leakage boundary conditions at the surface, from $\Psi_R(r|n)$ we have

$$\langle n_R^1 \rangle = 1 + R^2 - e^{-R} - \frac{R^4 e^{-r_e}}{4r_e^3} - \frac{R^4}{2r_e^2}. \tag{96}$$

IV. CONCLUSIONS

In this paper, we have examined the dynamics of exponential flights and their relation with the linear Boltzmann equation, a subject that arises in many areas of Physics or Biology. In particular, we have focused on $i)$ the propagator $\Psi(r, n)$, which describes the ensemble evolution of the transported particles as a function of the number of collisions, and $ii)$ the collision density $\Psi(r)$, which is related to the particle equilibrium distribution. Moreover, the connection between the number of collisions and time has been examined.

We have provided the framework for a generic d-dimensional setup, which allows emphasizing the key role of d in determining the properties of $\Psi(r, n)$ and $\Psi(r)$. In this context, we have shown that knowledge of $\Psi(r)$ formally allows deriving the moments of the residence times and number of collisions within a given volume. The role of boundary conditions has been explored by considering leakages from a given domain.

We have then provided specific results for $d = 1, 2, 3$ and 4 for infinite as well as bounded domains, and for absorbing or purely scattering media. A number of new results have been derived. The case $d = 1$ has been considered as a prototype model of exponential flights along a straight line, where only two directions (forward or backward) are possible. Due to this simplification, most quantities can be explicitly derived. The case $d = 2$ could provide a realistic description of migration on a surface, and has been analyzed in detail: despite the calculations being non trivial, in some cases explicit analytical results can be obtained. In particular, we have provided an expression for the collision density, which, coupled with the method of images, may be useful for describing the spread of chemical and biological species on unbounded as well as bounded surfaces. The case $d = 3$ is key in most real-world applications, such as the propagation of neutrons or photons in matter. Unfortunately, this case turns out to be hardly amenable to closed-form analytical formulas, and most results concern the asymptotic behavior of the particles, either close to or far from the source. Finally, the case $d = 4$ has been considered for the sake of completeness. In all such cases, Monte Carlo simulations have been performed so as to validate the proposed results and support the analysis of the asymptotic behavior. A good agreement is found between theoretical predictions and numerical simulations.

Acknowledgments

Appendix A: Spatial moments

We begin by computing the m-th coefficient of the Taylor expansion of $z^{1-d/2} J_{d/2-1}(rz)$ with respect to z, which reads

$$\frac{1}{m!} \frac{\partial^m}{\partial z^m} \left[z^{1-d/2} J_{d/2-1}(rz) \right]_{z=0} = \frac{i^m \left(\frac{r}{2} \right)^{\frac{d}{2}+m-1}}{\Gamma\left(1 + \frac{m}{2}\right) \Gamma\left(\frac{d+m}{2}\right)}, \tag{A1}$$

for even m, and zero otherwise. Apply now the m-th derivative to a function $f(z)$ such that $f(r)$ has a spherical symmetry. Recalling then the definition of the moment $\langle r^m \rangle$ from Eq. (36), we have

$$\frac{1}{m!} \frac{\partial^m}{\partial z^m} [f(z)]_{z=0} = \frac{i^m 2^{1-\frac{d}{2}-m} (2\pi)^{\frac{d}{2}}}{\Gamma\left(1 + \frac{m}{2}\right) \Gamma\left(\frac{d+m}{2}\right)} \frac{\langle r^m \rangle}{\Omega_d}. \tag{A2}$$

Rearranging the coefficients, we can finally express the spatial moments of $f(r)$ in terms of the m-th z-derivative of $f(z)$, namely,

$$\langle r^m \rangle = \frac{\sqrt{\pi} \Gamma\left(\frac{d+m}{2}\right)}{\Gamma\left(\frac{d}{2}\right) \Gamma\left(\frac{1+m}{2}\right)} \frac{\partial^m}{\partial (iz)^m} [f(z)]_{z=0}. \tag{A3}$$

Appendix B: Collision density for $d = 2$

In order to find the collision density associated to the free propagator, we begin by decomposing the sum over the collisions n into even and odd index, i.e.,

$$\Psi(r) = \lim_{N \to \infty} \left[\sum_{n\,even} \Psi(r|n) + \sum_{n\,odd} \Psi(r|n) \right]. \tag{B1}$$

Then, by remarking that for even n

$$\Psi_{even}(z) = \sum_{n\,even} \Psi(z|n) = \frac{1 - \left(1 + z^2\right)^{-N}}{z^2}, \tag{B2}$$

we get

$$\Psi_{even}(r) \simeq \frac{\log(\sqrt{N}) - \log(r)}{2\pi} \tag{B3}$$

for large N. We have neglected a constant term of the kind $[\log(2) - \gamma/2]/(2\pi)$, which is small compared to $\log(N)$.

For odd n, we can use the series representation

$$\Psi(r|n_{odd}) = \sum_{k\,even} \frac{2^{-2-k} \Gamma\left(2 - \frac{n}{2}\right) \Gamma\left(-1 + \frac{n}{2}\right)}{\pi \Gamma\left(1 + \frac{k}{2}\right) \Gamma\left(2 + \frac{k}{2} - \frac{n}{2}\right) \Gamma\left(\frac{n}{2}\right)} r^k +$$

$$\sum_{\substack{(n-k)\,even \\ k \geq n-2}} \frac{2^{-2-k} \Gamma\left(2 - \frac{n}{2}\right)}{\pi \Gamma\left(1 + \frac{k}{2}\right) \Gamma\left(2 + \frac{k}{2} - \frac{n}{2}\right)} r^k. \tag{B4}$$

Now, carrying out the double sum over odd n and over k, from Eq. (B4) we get

$$\Psi_{odd}(r) \simeq \frac{\log(\sqrt{N}) + \frac{e^{-r}}{r} + \mathrm{E}i\left(-r\right) - \log(r)}{2\pi}, \tag{B5}$$

for large N. Again, to obtain this result we have neglected a constant term of the kind $[\log(2) - \gamma/2]/(2\pi)$, which is small compared to $\log(N)$.

Hence, by summing up we finally obtain

$$\Psi(r) \simeq \frac{\log(N) + \frac{e^{-r}}{r} + \mathrm{E}i\left(-r\right) - 2\log(r)}{2\pi}. \tag{B6}$$

[1] B. D. Hughes, *Random walks and random environments* Vol. I (Clarendon Press, Oxford, 1995).

[2] G. H. Weiss, *Aspects and applications of the random walk* (North Holland Press, Amsterdam, 1994).

[3] W. Feller, *An introduction to probability theory and its applications*, 3rd edition (Wiley, New York, 1970).

[4] R. Metzler and J. Klafter, Phys. Rep. **339**, 1 (2000).

[5] J. Dutka, Arch. Hist. Exact Sci. **32**, 351 (1985).

[6] G. I. Bell and S. Glasstone, *Nuclear reactor theory* (Van Nostrand Reinhold, 1970).

[7] M. Weinberg and E. P. Wigner, *The physical theory of neutron chain reactors* (University of Chicago Press, 1958).

[8] C. Cercignani, *The Boltzmann equation and its applications* (Springer, 1988).

[9] H. T. Hillen and G. Othmer, Siam J. Appl. Math **61**, 751 (2000).

[10] M. Abramowitz and I. A. Stegun (Eds.), *Handbook of Mathematical Functions with Formulas, Graphs, and Mathematical Tables*, 9th edition (Dover, NY, 1972).

[11] J. C. J. Paasschens, Phys. Rev. E **56**, 1135 (1997).

[12] E. Orsingher and A. De Gregorio, J. Theor. Probab. **20**, 769 (2007).

[13] A. D. Kolesnik, J. Stat. Phys. **131**, 1039 (2008).

[14] G. Le Caër, J. Stat. Phys. **140**, 728 (2010).

[15] S. Redner, *A Guide to First-Passage Processes* (Cambridge University Press, Cambridge, 2001).

[16] I. Freund, Phys. Rev. A **45**, 8854 (1992).

[17] G. Placzek and W. Seidel, Phys. Rev. **72**, 550 (1947).

[18] A. M. Berezhkovskii, V. Zaloj, and N. Agmon, Phys. Rev. E **57**, 3937 (1998).

[19] G. Milton Wing, *An introduction to transport theory* (Wiley, NY, 1962).

[20] K. M. Case and P. F. Zweifel, *Linear transport theory* (Addison-Wesley, Reading, 1967).

[21] W. Stadje, J. Stat. Phys. **46**, 207 (1987).

[22] B. Conolly and D. Roberts, Eur. J. Op. Res. **28**, 308 (1987).